

Diffusion Coefficients Estimated by Dynamic Fluorescence Quenching at High Pressure: Pyrene, 9,10-Dimethylanthracene, and Oxygen in *n*-Hexane

M. Okamoto¹

Received May 29, 2001

The fluorescence quenching of pyrene (PY) by carbon tetrabromide (CBr₄) at pressures of up to 400 MPa in *n*-hexane was investigated. It was found that the fluorescence quenching is not fully, but nearly, diffusion-controlled. From the pressure-induced solvent viscosity dependence, the quenching rate constant, k_q , was separated into the contributions of the bimolecular rate constant in the solvent cage, k_{bim} , and that for diffusion, k_{diff} . Using the values of k_{diff} separated, together with those of the diffusion coefficient of CBr₄, the diffusion coefficients of PY were successfully estimated. This analysis was applied to the quenching systems of 9,10-dimethylanthracene (DMEA)/CBr₄ and of PY/O₂ and DMEA/O₂ that were studied previously. Using the values of k_{diff} for these systems, together with those of the corresponding diffusion coefficients of the fluorophore or quencher, the diffusion coefficients of DMEA and O₂ were also evaluated. Based on the results, the pressure-induced solvent viscosity, η , dependence on the diffusion coefficients is discussed.

KEY WORDS: diffusion coefficient; 9-10-dimethylanthracene; fluorescence quenching, high pressure; pyrene, oxygen.

1. INTRODUCTION

According to the diffusion model, the rate constant, k_{diff} , for the bimolecular diffusion-controlled reaction between the fluorescence state of M, M* and the quencher, Q, is given by Eq. (1) for a solvent with the relative diffusion

¹ Faculty of Engineering and Design, Kyoto Institute of Technology, Matsugasaki, Sakyo-ku, Kyoto 606-8585, Japan. E-mail: okamoto@hie1.kit.ac.jp

coefficient, $D_{M^*Q}(=D_{M^*}+D_Q)$ when the transient terms can be neglected [1-4]:

$$k_{\text{diff}} = 4\pi r_{M^*Q} D_{M^*Q} N_A / 10^3 \quad (1)$$

where r_{M^*Q} and N_A are the encounter distance ($=r_{M^*}+r_Q$; the sum of the radius of M^* and Q) and Avogadro's number, respectively. In a continuum medium of viscosity, η (in Poise: $1 \text{ P} = 0.1 \text{ Pa} \cdot \text{s}$), k_{diff} is given by the Debye equation [Eq. (2)], which can be derived from Eq. (1), in which r_{M^*} is assumed to be equal to r_Q , together with the Stokes-Einstein equation [1-4]:

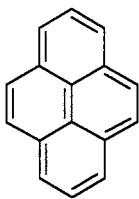
$$k_{\text{diff}} = 8RT / (\alpha\eta) \quad (2)$$

In Eq. (2), $\alpha = 2000$ and 3000 for the slip and stick boundary limits, respectively [1-4].

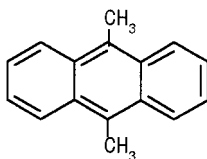
The fluorescence of some aromatic molecules is efficiently quenched by oxygen and carbon tetrabromide (CBr_4) in liquid solution [5-10] and often believed to be diffusion-controlled. The quenching rate constant, k_q , is about an order of $10^{10} \text{ M}^{-1} \cdot \text{s}^{-1}$ in nonviscous solvents, which is approximately equal to the rate constant for diffusion, k_{diff} , calculated by Eqs. (1) and (2). However, the discrepancy between k_q and k_{diff} is significantly large, depending on the solvents used as well as the fluorophore/quencher pairs. One of the reasons for this discrepancy may be attributed to the quenching mechanism, which is assumed to be diffusion-controlled.

Recently, the fluorescence quenching by polybromoethanes and CBr_4 of pyrene (PY) [11, 12] and by oxygen and CBr_4 of 9,10-dimethylanthracene (DMEA), benzo[a]pyrene (BZ[a]PY), and PY [13-15] at high pressure was examined and led to the conclusion that the quenching is not fully, but nearly, diffusion-controlled. The contribution of diffusion to the quenching was satisfactorily interpreted by a kinetic scheme via an encounter complex, followed by the formation of an exciplex in the solvent cage. By the analysis of the pressure-induced solvent viscosity dependence, the observed quenching rate constant, k_q , was separated into the contributions of the rate constant for the bimolecular reaction in the solvent cage, k_{bim} , and that for diffusion, k_{diff} . The separation of k_{diff} involved in the quenching processes leads to the evaluation of the diffusion coefficient of the fluorophore or quencher according to Eq. (1) when either is known. On the basis of this, the fluorescence quenching of BZ[a]PY by oxygen and CBr_4 was examined [14], and the diffusion coefficients of CBr_4 and O_2 were successfully evaluated according to Eq. (1) by using both the k_{diff} and the diffusion coefficient of BZ[a]PY at high pressure that were measured by Dymond and Woolf [16].

In this work, the rate constant, k_q , for the fluorescence quenching by CBr_4 of PY was measured at pressures up to 400 MPa, and k_{diff} involved in the quenching processes was separated. With the values of k_{diff} separated, together with those of the diffusion coefficient of CBr_4 [14], the diffusion coefficient of PY was evaluated as a function of pressure. The diffusion coefficient of DMEA was also evaluated by using the data reported previously [10]. Furthermore, the diffusion coefficient of O_2 was reevaluated by using the k_{diff} for the PY/ O_2 [15] and DMEA/ O_2 [10, 13] quenching systems. The structures of PY and DMEA are shown below:



PY



DMEA

2. EXPERIMENTAL

Pyrene (PY) (Wako Pure Chemicals Ltd.; guaranteed grade) was chromatographically tested twice on silica gel (200 mesh), then developed and eluted with pentane, and followed by recrystallization from ethanol. Carbon tetrabromide (CBr_4) (Wako Pure Chemicals Ltd.; guaranteed grade) was purified by sublimation twice under reduced pressure. The spectroscopic grade of *n*-hexane (Merck) was used without further purification.

Fluorescence decay curve measurements at high pressure were performed using a 0.3-ns pulse from a PRA LN103 nitrogen laser for excitation (337.1 nm/ $< 5 \mu\text{J}$ per pulse by ND filters), which was operated with a repetition of 10 Hz. The fluorescence intensities monitored at 382 nm were measured by a Hamamatsu R1635-02 photomultiplier through a Ritsu MC-25NP monochromator and the resulting signal accumulated 128 times and averaged was digitized using a LeCroy 9362 digitizing oscilloscope. The pulse width measured using this system was about 3 ns (HV for PMT = -700 V). All data were analyzed using a NEC 9801 microcomputer, which was interfaced to the digitizer. The details on the associated high-pressure techniques have been described elsewhere [17].

The concentration of PY for the fluorescence lifetime measurements was lower than 0.1 in absorbance (1-cm cell) at the maximum absorption wavelength to minimize the reabsorption effects. The sample solution was deoxygenated with bubbling nitrogen gas under a nitrogen atmosphere for 20 min. The change in the concentration of carbon tetrabromide with

bubbling was corrected by weighing the sample solution. The increase in the concentration due to the application of high pressure was corrected by using the compressibility of the solvent [18–20].

The temperature was controlled at $25 \pm 0.2^\circ\text{C}$. The pressure was measured with a Minebea STD-5000K strain gauge or a calibrated manganin wire.

3. RESULTS

3.1. Quenching Rate Constant, k_q

Fluorescence quenching was measured in the absence and presence of CBr_4 in *n*-hexane at 25°C . The decay curves were satisfactorily analyzed by a single-exponential function for all conditions examined. The lifetime evaluated does not depend on the laser shots irradiated for accumulation. The values of the lifetime, τ_f^0 , in the absence of the quencher are in good agreement with those reported previously [21]. The quenching rate constant, k_q , was determined by

$$(1/\tau_f) - (1/\tau_f^0) = k_q[\text{CBr}_4] \quad (3)$$

where τ_f represents the fluorescence lifetime in the presence of the quencher. The plots of $1/\tau_f$ against the concentration of CBr_4 are shown in Fig. 1. The values of k_q were determined from the least-squares slope of the plot according to Eq. (3) and are listed in Table I, together with the solvent viscosity, η [18–20].

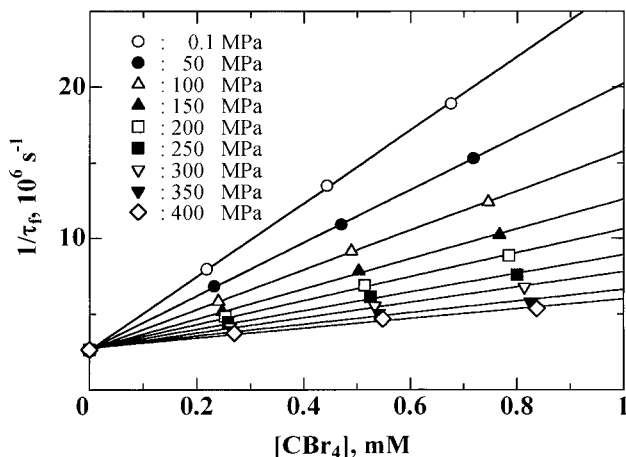


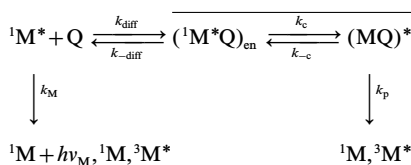
Fig. 1. Plots of $1/\tau_f$ versus the concentration of carbon tetrabromide, $[\text{CBr}_4]$, in *n*-hexane at 25°C .

Table I. Solvent Viscosity, η , and Quenching Rate Constant, k_q , for PY/CBr₄ in *n*-Hexane at 25°C

P (MPa)	η (10^{-3} Pa·s)	k_q (10^{10} M ⁻¹ ·s ⁻¹)
0.1	0.294	2.47 ± 0.15
50	0.472	1.75 ± 0.11
100	0.650	1.33 ± 0.08
150	0.849	1.03 ± 0.07
200	1.063	0.82 ± 0.05
250	1.310	0.66 ± 0.04
300	1.610	0.54 ± 0.04
350	1.948	0.44 ± 0.03
400	2.368	0.36 ± 0.03

3.2. Determination of the Rate Constant for Diffusion, k_{diff}

For fluorescence quenching by a heavy atom quencher (Q) of pyrene ($^1M^*$) in liquid solution, the quenching occurs via an exciplex (MQ)^{*} which is formed from an encounter complex ($^1M^*Q$)_{en} between $^1M^*$ and Q in the solvent cage as follows [12]:

**Scheme I**

The bar indicates the solvent cage. Scheme I was also successfully applied to fluorescence quenching systems in liquid [11–15] and supercritical carbon dioxide [13]. In Scheme I, when the rate constant for diffusion, k_{diff} , is expressed by Eq. (2) (α is replaced by α^{ex}), one may derive Eq. (4).

$$\frac{1}{k_q} = \left(\frac{k_p + k_{-c}}{k_c k_p} \right) \left(\frac{k_{-diff}}{k_{diff}} \right) + \frac{\alpha^{\text{ex}}}{8RT} \eta \quad (4)$$

In Eq. (4), the pressure dependence of $k_{\text{diff}}/k_{-diff}$ is given by that of the radial distribution function, $g(r_{M^*Q})$, at the closest approach distance (the encounter distance) with hard spheres, r_{M^*Q} ($= r_{M^*} + r_Q$) [12], where r_{M^*}

and r_Q are the hard-sphere radii of $^1M^*$ and Q , respectively. Using this relation, Eq. (5) can be derived:

$$\frac{\gamma}{k_q} = \left(\frac{k_p + k_{-c}}{k_c k_p} \right) \left(\frac{k_{-diff}}{k_{diff}} \right)_0 + \frac{\alpha^{ex}}{8RT} \gamma \eta \quad (5)$$

where γ is the ratio of $g(r_{M^*Q})$ at P (in MPa) to that at 0.1 MPa, $g(r_{M^*Q})/g(r_{M^*Q})_0$, and $(k_{-diff}/k_{diff})_0$ is k_{-diff}/k_{diff} at 0.1 MPa [22]. According to Eq. (5), the plot of γ/k_q against $\gamma\eta$ should be linear when $(k_p + k_{-c})/(k_c k_p)$ is independent of pressure.

The plots of γ/k_q against $\gamma\eta$ for PY/CBr₄ are shown in Fig. 2, together with that for PY/O₂ [15] for comparison. The plots shown in Fig. 2 are approximately linear with positive intercepts, indicating that the quenching competes with diffusion, and, hence, $(k_p + k_{-c})/k_c k_p$ is approximately independent of $\gamma\eta$, that is, pressure. These observations are consistent with those found for the fluorescence quenching systems studied previously [12–15]. The values of α^{ex} and the bimolecular rate constant, k_{bim}^0 , defined by

$$k_{bim}^0 = \left(\frac{k_c k_p}{k_p + k_{-c}} \right) \left(\frac{k_{diff}}{k_{-diff}} \right)_0 \quad (6)$$

were determined from the least-squares slope and intercept of the plot (Fig. 2), respectively, and are summarized in Table II together with the values reported previously for some systems. As shown in Table II, the

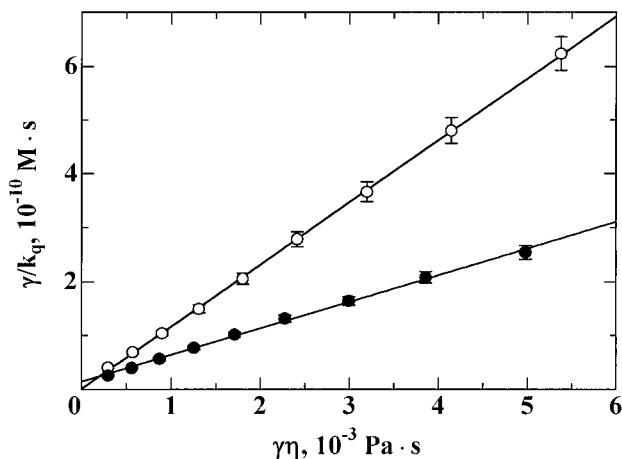


Fig. 2. Plots of γ/k_q versus $\gamma\eta$ for PY/CBr₄ (○) and PY/O₂ (●) [15] in *n*-hexane at 25°C.

Table II. Values of α^{ex} and k_{bim}^0 for the Fluorophore/Quencher Pairs in *n*-Hexane at 25°C

	α^{ex}	k_{bim}^0 ($10^{10} M^{-1} \cdot s^{-1}$)
PY/CBr ₄ ^a	2280 ± 20	69 ± 96
PY/O ₂ ^b	980 ± 20	6.9 ± 0.2
DMEA/CBr ₄ ^c	1820 ± 30	5.5 ± 0.9
DMEA/O ₂ ^c	940 ± 20	5.4 ± 0.8
BZ[a]PY/CBr ₄ ^d	1980 ± 200	7.0 ± 0.5
BZ[a]PY/O ₂ ^d	900 ± 20	7.2 ± 0.1

^a This work.^b Ref. 15.^c Ref. 13.^d Ref. 14.

value of k_{bim}^0 for PY/CBr₄ has a large error. Probably, it falls in similar magnitude to the values for DMEA/CBr₄ and BZ[a]PY/CBr₄, judging from the values of k_{bim}^0 shown in Table II.

3.3. Diffusion Coefficients of Pyrene (PY) and 9,10-Dimethylantracene (DMEA)

The observed quenching rate constant, k_q , was separated into the contributions of k_{bim} and k_{diff} as described in the previous section. The values of k_{diff} for PY/CBr₄ that were determined from α^{ex} and the solvent viscosity, η , according to Eq. (2), are summarized in Table III. Using the values of k_{diff} , we can evaluate the relative diffusion coefficient, D_{M^*Q} ($= D_{M^*} + D_Q$), according to Eq. (1) since the van der Waals radii are calculated by the method of Bondi [24]. The values of $D_{M^*} + D_Q$ for PY/CBr₄ are listed in Table III, together with those of D_Q for CBr₄ determined by the fluorescence quenching for the BZ[a]PY/CBr₄ system [14]. The values of D_{M^*} for PY thus determined are also listed in Table III.

In the previous work, we studied the fluorescence quenching of DMEA by CBr₄ and determined α^{ex} ($= 1820 \pm 30$) in *n*-hexane (see Table II) [13]. Using the values of k_{diff} , together with those of D_Q for CBr₄, the values of D_{M^*} for DMEA were evaluated. The results are listed in Table IV.

3.4. Diffusion Coefficient of Oxygen

We studied previously the fluorescence quenching of PY and DMEA by oxygen in *n*-hexane. The values of α^{ex} for these systems are summarized in Table II. Using α^{ex} and η , k_{diff} was calculated, and the values of D_Q for O₂, together with those of D_{M^*} for PY and DMEA estimated in the previous

Table III. Rate Constants for Diffusion, k_{diff} , and the Parameters for Diffusion Associated with the Fluorescence Quenching for PY/CBr₄ in *n*-Hexane at 25°C^a

P (MPa)	k_{diff} ($10^{10} M^{-1} \cdot s^{-1}$)	$D_{\text{PY}^*} + D_{\text{CBr}_4}$ ($10^{-9} \text{m}^2 \cdot \text{s}^{-1}$) ^b	D_{CBr_4} ($10^{-9} \text{m}^2 \cdot \text{s}^{-1}$) ^c	D_{PY^*} ($10^{-9} \text{m}^2 \cdot \text{s}^{-1}$)
0.1	2.96 ± 0.26	6.13	4.41	1.72 ± 0.98
50	1.84 ± 0.16	3.82	2.54	1.28 ± 0.57
100	1.34 ± 0.12	2.77	1.83	0.94 ± 0.41
150	1.02 ± 0.09	2.12	1.38	0.74 ± 0.31
200	0.82 ± 0.08	1.70	1.09	0.61 ± 0.25
250	0.66 ± 0.06	1.38	0.89	0.48 ± 0.20
300	0.54 ± 0.05	1.12	0.75	0.38 ± 0.17
350	0.45 ± 0.04	0.93	0.63	0.30 ± 0.14
400	0.36 ± 0.04	0.76		

^a The van der Waals radii of PY and CBr₄ were estimated to be 0.351 and 0.289 nm, respectively, by the method of Bondi [24].

^b Error was evaluated to be about ± 3%.

^c Assumed that $D_{\text{BZ[a]PY}^*} = D_{\text{BZ[a]PY}}$ [14].

section, were evaluated. The results are shown in Table V, together with the values of D_Q for O₂ determined from the BZ[a]PY/O₂ quenching system [14]. It is noted in Table V that the values of D_Q for O₂, which were estimated from three quenching systems of fluorophore/O₂, are approximately equal at each pressure.

Table IV. Rate Constants for Diffusion, k_{diff} , and the Parameters for Diffusion Associated with the Fluorescence Quenching for DMEA/CBr₄ in *n*-Hexane at 25°C^a

P (MPa)	k_{diff} ($10^{10} M^{-1} \cdot s^{-1}$)	$D_{\text{DMEA}^*} + D_{\text{CBr}_4}$ ($10^{-9} \text{m}^2 \cdot \text{s}^{-1}$) ^b	D_{CBr_4} ($10^{-9} \text{m}^2 \cdot \text{s}^{-1}$) ^c	D_{DMEA^*} ($10^{-9} \text{m}^2 \cdot \text{s}^{-1}$)
0.1	3.70 ± 0.07	7.51	4.41	3.09 ± 1.02
50	2.30 ± 0.04	4.67	2.54	2.13 ± 0.60
100	1.67 ± 0.03	3.39	1.83	1.56 ± 0.44
150	1.28 ± 0.03	2.60	1.38	1.22 ± 0.33
200	1.02 ± 0.02	2.07	1.09	0.99 ± 0.23
250	0.83 ± 0.02	1.68	0.89	0.79 ± 0.22
300	0.68 ± 0.02	1.37	0.75	0.63 ± 0.18
350	0.56 ± 0.01	1.13	0.63	0.50 ± 0.15
400	0.46 ± 0.01	0.93		

^a The van der Waals radii of DMEA and CBr₄ were estimated to be 0.365 and 0.289 nm, respectively, by the method of Bondi [24].

^b Error was evaluated to be about ± 3%.

^c Assumed that $D_{\text{BZ[a]PY}^*} = D_{\text{BZ[a]PY}}$ [14].

Table V. Diffusion Coefficients of Oxygen Estimated from the Fluorescence Quenching for PY/O₂, DMEA/O₂, and BZ[a]PY/O₂ in *n*-Hexane at 25°C, Coupled with the Diffusion Coefficients for PY*, DMEA*, and BZ[a]PY*, Respectively

<i>P</i> (MPa)	<i>D</i> _{O₂} (10 ⁻⁹ m ² ·s ⁻¹)		
	PY/O ₂ ^a	DMEA/O ₂ ^b	BZ[a]PY/O ₂ ^c
0.1	15.7 ± 1.5	14.6 ± 1.6	16.4
50	9.62 ± 0.90	8.87 ± 0.93	10.0
100	6.95 ± 0.65	6.43 ± 0.68	7.27
150	5.30 ± 0.50	4.90 ± 0.51	5.54
200	4.21 ± 0.40	3.90 ± 0.41	4.42
250	3.44 ± 0.32	3.17 ± 0.33	3.59
300	2.81 ± 0.27	2.61 ± 0.28	2.94
350	2.33 ± 0.22	2.17 ± 0.23	2.45

^a This work.^b *k*_{diff} was taken from Ref. 13.^c Assumed that *D*_{BZ[a]PY*} = *D*_{BZ[a]PY} [14].

The values of *D*_{M*} for PY and DMEA can be also evaluated by using *D*_Q for O₂ as a reference [14], together with *D*_{M*Q} for PY/O₂ and DMEA/O₂. They are consistent with those estimated using *D*_Q for CBr₄ as a reference, although the former estimation by the reference of *D*_Q for O₂ leads to larger errors.

4. DISCUSSION

4.1. Rate Constant for Diffusion, *k*_{diff}

The diffusion coefficient *D*_{*i*} (*i* = ¹M* or Q) for the solute molecule, *i*, in a given solvent is expressed by the Einstein equation

$$D_i = k_B T / \zeta_i \quad (7)$$

where ζ_i and k_B are the friction coefficient and the Boltzmann constant, respectively. Since the hydrodynamic friction, ζ_i^H , for the solute molecule of the spherical radius, r_i , in a continuum medium with viscosity, η , is given by $\zeta_i^H = f_i \pi r_i \eta$ (Stokes' law), one can obtain the Stokes–Einstein (SE) equation,

$$D_i^{SE} = k_B T / (f_i \pi r_i \eta) \quad (8)$$

where $f_i = 4$ and 6 for the slip and stick boundary limits, respectively. The SE equation has been often found to break down for measurements of

the diffusion coefficient at 0.1 MPa by changing solvent [3, 25, 26]. In previous publications [12–15], the solvent-viscosity dependence of k_{diff} induced by pressure was successfully described for several quenching systems on the basis of an empirical equation proposed by Spagnol and Wirtz [2, 27, 28]. According to the Spagnol–Wirtz (SW) equation, the diffusion coefficient, D_i^{SW} , is expressed by

$$D_i^{\text{SW}} = k_B T / (6\pi f_i^{\text{SW}} r_i \eta) \quad (9)$$

where f_i^{SW} represents a microfriction factor and is given by

$$f_i^{\text{SW}} = (0.16 + 0.4r_i/r_s)(0.9 + 0.4T_s^r - 0.25T_i^r) \quad (10)$$

In Eq. (10), the first parenthetical quantity depends only on the solute-to-solvent size ratio, (r_i/r_s), which can be calculated using the van der Waals radii of the solute and solvent molecules. The second parenthetical quantity involves the reduced temperatures, T_s^r and T_i^r , of the solvent and solute, respectively, which can be calculated using the melting point, T_{mp} , and boiling point, T_{bp} , of the solvent or solute at the experimental temperature [2, 27, 28]. From the SW approximation, one can derive Eq. (11):

$$k_{\text{diff}} = \frac{2RT r_{M^*Q}}{3000\eta} \left(\frac{1}{f_{M^*}^{\text{SW}} r_{M^*}} + \frac{1}{f_Q^{\text{SW}} r_Q} \right) \quad (11)$$

By comparison with Eq. (2), α^{SW} is given by

$$\alpha^{\text{SW}} = \frac{1.2 \times 10^4}{r_{M^*Q}} \left(\frac{1}{f_{M^*}^{\text{SW}} r_{M^*}} + \frac{1}{f_Q^{\text{SW}} r_Q} \right)^{-1} \quad (12)$$

The values of $\alpha^{\text{SW}}(\text{trunc})$ and $\alpha^{\text{SW}}(\text{full})$ for PY/CBr₄ calculated according to Eq. (12) [29] are summarized in Table VI, together with those reported previously for some fluorophore/quencher pairs in *n*-hexane [13–15]. In Table VI, the values of $\alpha^{\text{SW}}(\text{full})$ for the fluorophore/oxygen pairs are not included since they have negative values as described previously [13–15]. By comparison of the results in Table II with those in Table VI, α^{ex} is in good agreement with α^{SW} for PY/CBr₄ as seen for the other fluorophore/quencher pairs listed in Table VI.

4.2. Diffusion Coefficients at 0.1 MPa

To our knowledge, there are no experimental data of the diffusion coefficient of PY and DMEA in *n*-hexane at high pressures as well as at 0.1 MPa. The diffusion coefficients, $D_i^{\text{SW}}(\text{trunc})$ and $D_i^{\text{SW}}(\text{full})$, evaluated

Table VI. Values of $\alpha^{\text{SW}}(\text{trunc})$ and $\alpha^{\text{SW}}(\text{full})$ for the Fluorophore/Quencher Pairs in *n*-Hexane at 25°C

	$\alpha^{\text{SW}}(\text{trunc})$	$\alpha^{\text{SW}}(\text{full})$
PY/CBr ₄ ^a	1798	2431
PY/O ₂ ^b	1229	
DMEA/CBr ₄ ^c	1730	2340
DMEA/O ₂ ^c	1171	
BZ[a]PY/CBr ₄ ^d	1795	2420
BZ[a]PY/O ₂ ^d	1232	

^a This work.^b Ref. 15.^c Ref. 13.^d Ref. 14.

by the SW equation [Eq. (9)] were 3.26×10^{-9} and $2.46 \times 10^{-9} \text{ m}^2 \cdot \text{s}^{-1}$, respectively, for PY, and 3.06×10^{-9} and $2.32 \times 10^{-9} \text{ m}^2 \cdot \text{s}^{-1}$, respectively, for DMEA; they are in good agreement with the diffusion coefficients of PY and DMEA estimated by the present work (see Tables III and IV).

The diffusion coefficient for $i = \text{O}_2$, $D_{\text{O}_2}^{\text{SW}}(\text{trunc})$, was evaluated to be $10.8 \times 10^{-9} \text{ m}^2 \cdot \text{s}^{-1}$, which is compared with the 15.7×10^9 and $14.6 \times 10^9 \text{ m}^2 \cdot \text{s}^{-1}$ determined from the fluorescence quenching for PY/O₂ and DMEA/O₂, respectively. The values of D_{O_2} evaluated in this work are in good agreement with those obtained from BZ[a]PY/O₂ ($16.4 \times 10^{-9} \text{ m}^2 \cdot \text{s}^{-1}$) (see Table V). There are a few data of the diffusion coefficient for oxygen in some liquid solutions at 0.1 MPa. However, they are very scattered; for example, they are 9.0×10^{-9} and $6.7 \times 10^{-9} \text{ m}^2 \cdot \text{s}^{-1}$ in acetone [5, 30], 5.7×10^{-9} and $3.5 \times 10^{-9} \text{ m}^2 \cdot \text{s}^{-1}$ in benzene [5, 30], and 3.9×10^{-9} , 1.6×10^{-9} and $2.6 \times 10^{-9} \text{ m}^2 \cdot \text{s}^{-1}$ in ethanol [5, 31, 32]. Very recently, the D_{O_2} in *n*-hexane was reported to be $9.91 \times 10^{-9} \text{ m}^2 \cdot \text{s}^{-1}$ [33], which is approximately equal to that evaluated in this work.

Evans et al. [25, 26] have measured the diffusion coefficients of spherical solutes with different molecular sizes in some liquid solutions at 0.1 MPa using the Taylor dispersion technique, and found that $D_i \eta / T$ increases rapidly with a decrease in the size of the solute, r_w . The plots of D_i ($i = \text{tetradodecyltin}/\text{Dd}_4\text{Sn}$ to Ar) versus r_w^{-1} in *n*-hexane using their data are shown in Fig. 3 where the solid line was approximated by a polynomial of fourth order, together with the values of D_i observed and estimated for the solutes. It is noted in Fig. 3 that D_i for PY, DMEA, and O₂ in this work is close to the solid line. The evidence also supports the validity of the estimation of the diffusion coefficient by dynamic fluorescence quenching.

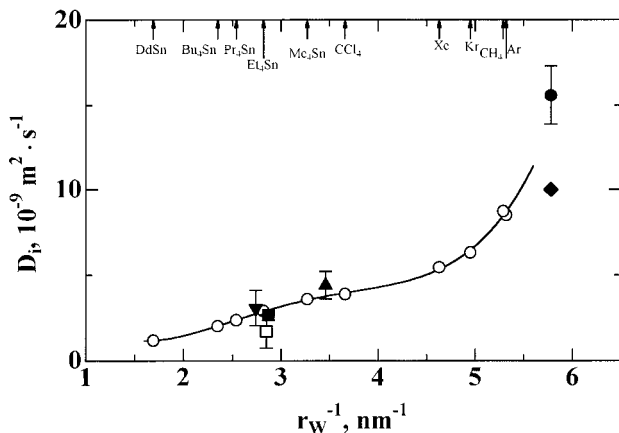


Fig. 3. Plots of D_i versus the inverse of the van der Waals radius, r_W^{-1} , in *n*-hexane at 25°C and 0.1 MPa. The values of D_i (i = tetradodecyltin/Dd₄Sn to Ar) (○) were taken from Refs. 25 and 26, and those of $D_{\text{BZ[a]PY}}$ (■) and D_{O_2} (◆) from Refs. 16 and 33, respectively. The value of D_{CBr_4} (▲) was evaluated from the dynamic fluorescence quenching of BZ[a]PY by CBr₄ [14]. The values of D_{PY^*} (□), D_{DMEA^*} (▼), and D_{O_2} (●) were evaluated in this work.

4.3. Pressure Dependence of the Diffusion Coefficient

As shown in the plots of D_i versus $1/\eta$, which is shown in Fig. 4, the diffusion coefficient, D_i , of PY, DMEA, and O₂ evaluated in this work decreases approximately inversely proportionally to the solvent viscosity induced by pressure. In fact, the approximately linear plots of the diffusion coefficient against $1/\eta$ have been observed for measurements of the mutual diffusion coefficient of some compounds in *n*-hexane [16] and also observed for those of the self-diffusion coefficient in several solvents [34–36].

The values of f_i in Eq. (8) determined from the slope of the plot of D_i against $1/\eta$ were 6.7 ± 0.5 , 3.8 ± 0.2 , and 1.7 ± 0.1 for PY, DMEA, and O₂, respectively (see Fig. 4). The value of f_i is close to the stick boundary limit ($f_i=6$) for PY, and nearly equal to the slip boundary limit ($f_i=4$) for DMEA. However, the f_i for O₂ is significantly lower than 4. These results indicate that f_i may be related to the size ratio of solute to solvent as seen in Fig. 3. It is also noted that the value of f_i evaluated in this work is close to $f_i^{\text{SW}} (= f_i/6)$ predicted by Eq. (10) except for $f_i^{\text{SW}}(\text{full})$ for O₂, suggesting that the SW equation gives a good approximation for the estimation of D_i for PY, DMEA, and O₂.

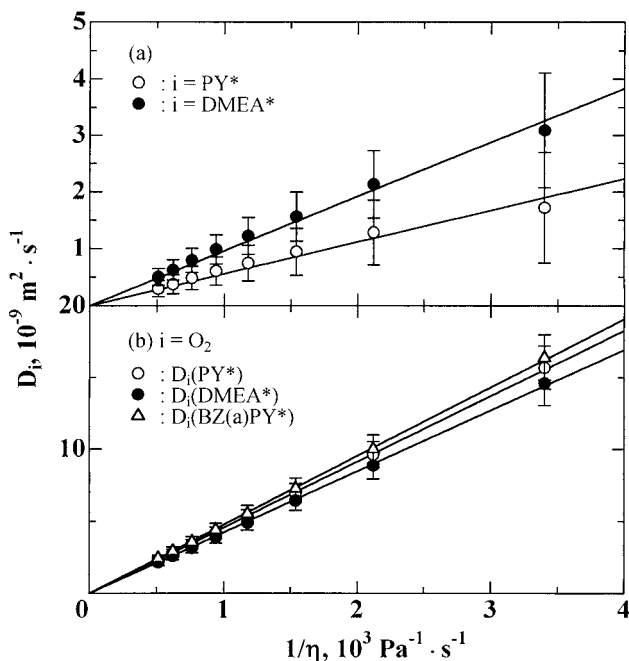


Fig. 4. Plots of D_i versus $1/\eta$ in *n*-hexane at 25°C: (a) $i = \text{PY}^*$ and DMEA^* , and (b) $i = \text{O}_2$, where $D_i(\text{PY}^*)$ and $D_i(\text{DMEA}^*)$ were evaluated from k_{diff} for the dynamic fluorescence quenching for PY/O_2 and DMEA/O_2 coupled with D_{PY^*} and D_{DMEA^*} , respectively (see text), and $D_i(\text{BZ[a]PY}^*)$ was taken from Ref. 14.

5. SUMMARY

It has been demonstrated that the fluorescence quenching by carbon tetrabromide (CBr_4) of pyrene (PY) is not fully, but nearly, diffusion-controlled. The contribution of diffusion to the quenching was successfully analyzed by Eq. (5), and the observed k_q was separated into the contributions of the bimolecular rate constant in the solvent cage, k_{bim} , and the rate constant for diffusion, k_{diff} . Using the values of k_{diff} thus separated, together with those of the diffusion coefficient, D_Q , for CBr_4 that were evaluated previously [14], the values of D_M^* for PY were evaluated at pressures up to 350 MPa according to Eq. (1). The analysis was applied to the quenching system of 9,10-dimethylanthracene (DMEA)/ CBr_4 [13], and the values of D_M^* for DMEA were also evaluated. Using k_{diff} determined from the fluorescence quenching rate constants for PY/O_2 [15] and DMEA/O_2 [10, 13], together with D_M^* for PY and DMEA estimated in this work, the values of

D_Q for oxygen were estimated. From these results, it has been shown that the fluorescence quenching by O_2 and CBr_4 gives a good estimation for the diffusion coefficients of PY, DMEA, and O_2 . It has also been shown that D_{M^*} for PY and DMEA and D_Q for O_2 are approximately inversely proportional to the pressure-induced solvent viscosity, η .

REFERENCES

1. J. B. Birks, *Photophysics of Aromatic Molecules* (Wiley-Interscience, New York, 1970), p. 518.
2. J. Saltiel and B. W. Atwater, *Advances in Photochemistry* (Wiley-Interscience, New York, 1987), Vol. 14, p. 1.
3. J. B. Birks, *Organic Molecular Photophysics* (Wiley, New York, 1973), p. 403.
4. S. A. Rice, in *Comprehensive Chemical Kinetics. Diffusion-Limited Reactions*, C. H. Bamford, C. F. H. Tripper, and R. G. Compton, eds. (Elsevier, Amsterdam, 1985), Vol. 25.
5. W. R. Ware, *J. Phys. Chem.* **66**:455 (1962).
6. W. R. Ware and J. S. Novros, *J. Phys. Chem.* **70**:3246 (1966).
7. T. M. Nemzek and W. R. Ware, *J. Chem. Phys.* **62**:477 (1975).
8. H. Yasuda, A. D. Scully, S. Hirayama, M. Okamoto, and F. Tanaka, *J. Am. Chem. Soc.* **112**:6847 (1990).
9. S. Hirayama, H. Yasuda, A. D. Scully, and M. Okamoto, *J. Phys. Chem.* **98**:4609 (1994).
10. M. Okamoto, F. Tanaka, and S. Hirayama, *J. Phys. Chem. A* **102**:10703 (1998).
11. M. Okamoto, *J. Phys. Chem. A* **104**:5029 (2000).
12. M. Okamoto, *J. Phys. Chem. A* **104**:7518 (2000).
13. M. Okamoto, O. Wada, F. Tanaka, and S. Hirayama, *J. Phys. Chem. A* **105**:566 (2001).
14. M. Okamoto and O. Wada, *J. Photochem. Photobiol. A Chem.* **138**:87 (2001).
15. M. Okamoto and F. Tanaka, submitted for publication.
16. J. H. Dymond and L. A. Woolf, *J. Chem. Soc. Faraday Trans. I* **78**:991 (1982).
17. M. Okamoto and H. Teranishi, *J. Phys. Chem.* **88**:5644 (1984).
18. P. W. Bridgman, *Proc. Am. Acad. Arts Sci.* **61**:57 (1926).
19. D. W. Brazier and G. R. Freeman, *Can. J. Chem.* **47**:893 (1969).
20. C. M. B. P. Oliveira and W. A. Wakeham, *Int. J. Thermophys.* **13**:773 (1992).
21. M. Okamoto and S. Sasaki, *J. Phys. Chem.* **95**:6548 (1991).
22. The radial distribution function, $g(r_{M^*Q})$, at the closest approach distance, $r_{M^*Q}(=r_{M^*}+r_Q)$, the sum of the radius of the hard-sphere solutes in a hard-sphere solvent with radius, r_s , is given by [23]

$$g(r_{M^*Q}) = \frac{1}{1-y} + \frac{3y}{(1-y)^2} \left(\frac{r_{red}}{r_s} \right) + \frac{2y^2}{(1-y)^3} \left(\frac{r_{red}}{r_s} \right)^2 \quad (A1)$$

where $r_{red} = r_{M^*}r_Q/r_{M^*Q}$, and y is the packing fraction, given in terms of the molar volume of the solvent, V_s , by

$$y = \frac{4N_A\pi r_s^3}{3V_s} \quad (A2)$$

By using the values of r_s , r_Q , and r_{M^*} estimated by the method of Bondi [24], together with the data on the solvent density [18–20], $g(r_{M^*Q})$ was calculated by Eq. (A1).

23. Y. Yoshimura and M. Nakahara, *J. Chem. Phys.* **81**:4080 (1984).

24. A. Bondi, *J. Phys. Chem.* **68**:441 (1964).
25. D. F. Evans, T. Tominaga, and C. Chan, *J. Solut. Chem.* **8**:461(1979).
26. D. F. Evans, T. Tominaga, and H. T. Davis, *J. Chem. Phys.* **74**:1298 (1981).
27. A. Spornol and K. Wirtz, *Z. Naturforsch.* **8A**:522 (1953).
28. A. Gierer and K. Wirtz, *Z. Naturforsch.* **8A**:532 (1953).
29. The values of f_i^{SW} (full) and f_i^{SW} (trunc) were evaluated by Eq. (10) and by neglecting the second parenthetical quantity in Eq. (10), respectively [2].
30. A. Schumpe and P. Lühring, *J. Chem. Eng. Data* **35**:24 (1990).
31. E. Sada, S. Kito, T. Oda, and Y. Ito, *Chem. Eng. J.* **10**:155 (1975).
32. A. Akgerman and J. L. Gainer, *Ind. Eng. Fundam.* **11**:373 (1972).
33. B. A. Kowert and N. C. Dang, *J. Phys. Chem. A* **103**:779 (1999).
34. J. Jonas, *Acc. Chem. Res.* **17**:74 (1984).
35. J. Jonas, D. Hasha, and S. G. Huang, *J. Phys. Chem.* **84**:109 (1980).
36. J. Jonas, D. Hasha, and S. G. Huang, *J. Chem. Phys.* **71**:3996 (1979).